Deep Learning for the Design of Toroidal Metasurfaces

Ting Chen, Tianyu Xiang, Tao Lei, and Mingxing Xu

***Abstract*—In recent years, the toroidal dipoles have had a profound impact on several fields including electromagnetism. However, the on-demand design of toroidal metasurfaces is still a very time-consuming process. In this paper, a method of neural network simulating the nonlinear relationship between the structural parameters of metasurfaces and its multipole scattered powers is proposed based on a deep learning algorithm. The forward network can quickly predict the scattered powers from input structural parameters, which can achieve an accuracy comparable to the electromagnetic simulations. In addition, with the required scattering spectrum as input, the appropriate parameters of the structure could be automatically calculated and then output by the inverse network which can achieve a low mean square error of 0.074 in training set and 0.18 in the test set. Compared with the conventional design process, the proposed deep learning model can guide the design of the toroidal dipole metasurface faster and pave the way for the rapid development of toroidal metasurfaces.**

***Index Terms*—Scattered power, toroidal dipole, deep learning, residual network, metasurface.**

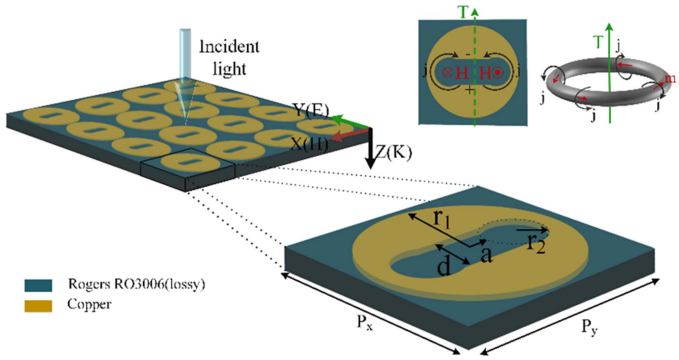

Fig. 1. Schematic diagram of TD and the toroidal metasurface. Poloidal currents flowing on a surface of a torus along its meridians create toroidal dipole moment T, which can be seen as a closed loop of magnetic dipoles arranged head-to-tail. Metal disc with a dumbbell-shaped aperture is the structural element of toroidal metamaterial.

I. Introduction

TOROIDAL dipole (TD), a fundamental member of the toroidal multipole family, was first proposed by Zel'dovich [1] in 1958 to interpret the parity nonconservation in the weak interaction. Unlike the conventional electric dipole (ED) and magnetic dipole (MD), TD is created by a current flowing along the meridian of a circular surface [2] as shown in the top right corner of Fig. 1, which can confine electromagnetic field in a small area and exhibits many special properties, such as circular dichroism [3], high Q-factor [4], etc. TD metasurfaces usually exhibit that the TD scattered power has been obviously enhanced to a measurable range while the scattered power of ED is strongly suppressed [5], [6]. In 2010, the resonant excitation of TD in metamaterial had been first demonstrated [7]. Afterwards, TD metasurfaces have attracted the attention of many researchers and been applied to a variety of fields such as electromagnetically induced transparency, highly sensitive sensors, modulators and absorbers [8], [9], [10], [11], [12], [13].

However, designing metasurfaces with TD resonance is often difficult. The traditional design methods of TD metasurfaces usually utilize electromagnetic simulation software such as HFSS, CST Microwave Studio, but the TD scattered power is not intuitive in the simulation software and further calculations are required for each candidate object. In addition, the conventional design approach involves a constant trial-and-error search in a large number of candidates of metasurfaces. Once the candidate object is changed, electromagnetic simulation and the calculation of scattered power need to be performed again, and the repetitive calculations require significant computational resources and designer efforts. Therefore, it is an important challenge of designing TD metasurfaces to obtain their multipole scattering characteristics directly from the given structural parameters of the metasurface that TD resonance evaluation can be performed quickly. In addition, the TD response is heavily dependent on the structural shape and size of the resonators. Conventional methods for designing metasurface with TD response and optimization still rely on the intuition, working experience and expertise of researchers. How to obtain the corresponding

Manuscript received 5 December 2022; revised 3 February 2023; accepted 9 March 2023. Date of publication 13 March 2023; date of current version 29 March 2023. This work was supported in part by the National Natural Science Foundation of China under Grant 61741104, in part by the Science and technology Foundation of Guizhou Province of China under Grant ZK [2021] 306, and in part by the Department of Education of Guizhou Province, Department of Education, Guizhou Province, under Grants KY [2017] 031 and KY [2020] 007. *(Corresponding author: Tao Lei.)*

Ting Chen and Mingxing Xu are with the School of Big Data and Computer Science, Guizhou Normal University, Guiyang, Guizhou 550003, China (e-mail: 20010230631@gznu.edu.cn; 21010230682@gznu.edu.cn).

Tianyu Xiang is with the School of Big Data and Computer Science, Guizhou Normal University, Guiyang, Guizhou 550003, China, and also with the College of Physical Science and Technology, Central China Normal University, Wuhan, Hubei 430079, China (e-mail: xty8587@gznu.edu.cn).

Tao Lei is with the School of Big Data and Computer Science, Guizhou Normal University, Guiyang, Guizhou 550003, China, and also with the State Key Laboratory of Millimeter Waves, School of Information Science and Engineering, Southeast University, Nanjing, Jiangsu 211189, China (e-mail: leitao2003101@gznu.edu.cn).

Digital Object Identifier 10.1109/JPHOT.2023.3256377

structure quickly according to the given multipole scattered power is the worthwhile research in the current.

Deep learning, a popular numerical computation method at the moment, demonstrates a superior ability to learn complex relationships between input and output data. Theoretically, deep learning can solve any nonlinear problem and has been widely used in areas such as pattern recognition, image processing, robotics, and data mining. In recent years, deep learning has been introduced to many physical systems by many scholars, such as plasmonic nanostructure design [14], [15], [16], digital coding metasurfaces [17], [18], intelligent metasurfaces [19] and other systems [20], [21], [22], [23], [24], [25]. Deep learning algorithms can easily learn the correlation between the structural parameters and electromagnetic response of material replacing the traditional time-consuming electromagnetic simulation and avoiding the complicated Maxwell solution process [26].

In 2018, J. Peurifoy et al. [27] proposed a neural network ANN that can approximate light scattering from multilayer nanoparticles. The ANN takes the thickness of each layer of nanoparticles as input and is able to output the transmission spectrum with an average error of less than 3% at each point after training. It is worth noting that the structure of the ANN is fixed after training, even if the structural parameters of the nanoparticles are changed the network structure does not need to be retrained. In addition, the training time of ANN is only 50 seconds, and the prediction accuracy can reach more than 95%. Compared with the traditional electromagnetic simulation, ANN has the advantage of higher efficiency, which saves the time cost of researchers to a large extent.

In 2019, S. So et al. [28] proposed a neural network with devised loss function to learn the correlation between the extinction spectra of ED and MD and core-shell nanostructure design. The neural network taking both material information and structural parameters as inverse design output achieved the on-demand design of independent ED and MD resonances. In 2020, L. Xu et al. [29] demonstrated the inverse design of a high quality (Q) metasurface consisting of two nanorods using deep learning, and the proposed tandem network can acquire high Q resonances with specific desired spectral locations, linewidths, and transmission amplitudes. However, the inverse design with the structural parameters and scattering spectrums of TD metasurfaces, to the best of our knowledge, has not been demonstrated

In this paper, a data-driven forward neural network (FNN) is innovatively applied to learn the nonlinear relationship between structural parameters and ED, MD and TD scattered powers in small sample data. Like most simulations do, the FNN is able to predict the scattered powers of metasurfaces from the design parameters. In addition, a reverse neural network (RNN) is proposed to fast design TD metasurfaces, which can directly obtain the appropriate metasurface from a given spectrum of ED, MD and TD scattered powers. To demonstrate the predictive capability of the proposed method, metasurfaces designs with arbitrary TD resonance are exhibited and the corresponding surface current and magnetic field distributions are simulated to further verify the TD responses. Compared with the traditional design method of parametric scanning and iterative verification, this method saves a lot of time of designers by eliminating the complex design and optimization process and provides an efficient way to design TD metasurfaces on demand.

TABLE I
THE RANGE OF THE FOUR GEOMETRIC PARAMETERS

Parameters	Max(mm)	Min(mm)	Step(mm)
r_1	8.2	1.2	0.5
r_2	4.2	0.5	0.5
a	7.4	0	0.2
d	8	0	0.2

II. DESIGN GOAL AND SETUPS

To demonstrate the feasibility of deep learning in TD metasurface, a randomly selected target structure consists of a disc resonator etched off a dumbbell shape is shown in Fig. 1. The disc resonator is fabricated from a copper sheet of 0.035 mm thickness and affixed to a dielectric substrate with permittivity $\varepsilon_\gamma = 6.5$. The periodicity of the meta-atom ($P_x = P_y$) is fixed as 18 mm, and the geometric parameters r_1, r_2, a and d of the resonator are selected as independent variables of this structure. Due to the fixed period of the structure and the shape of the resonator, parameters of the metal resonator are physically limited to the range shown in Table I. In addition, as shown in Fig. 1, several conditions are necessary in order to stay within the physical limits of the metasurface, $r_1 > (2r_2 + a)$ and $d < 2r_2$.

When a beam of linearly y-polarized light enters the metasurface normally, the density of the conducting current under different structures can be extracted from the electromagnetic simulation results by changing the variables. And then the scattered powers of the TD metasurface could be obtained according to the multiple scattering theory [30].

And the radiated powers of multipoles can be calculated from the following formulas:

$$I = \frac{2\omega^2}{3c^3}|P|^2 + \frac{2\omega^4}{3c^3}|M|^2 + \frac{2\omega^6}{3c^5}|T|^2 + \frac{\omega^6}{5c^5}|Q_e|^2 + \frac{\omega^6}{20c^5}|Q_m|^2 + o(\omega) \quad (1)$$

where the moments of traditional ED and MD are respectively represented as P and M, and the values can be obtained from the following equations:

$$P = \frac{1}{i\omega}\int j d^3r \quad (2)$$

$$M = \frac{1}{2c}\int (r \times j)\, d^3r \quad (3)$$

And the third term is the TD moment (T) form the follow:

$$T = \frac{1}{10c}\int \left[(r \cdot j)\, r + 2r^2 j\right] d^3r \quad (4)$$

The next fourth term expresses the radiated power of the electric quadrupoles (Q_e), and the fifth term is derived from the magnetic quadrupoles (Q_m). The last term indicates the higher-order correction. In all the above equations, c represents the speed of light, j is the current and r corresponds to the distance vector from the origin to the point (x, y, z). In order to reduce

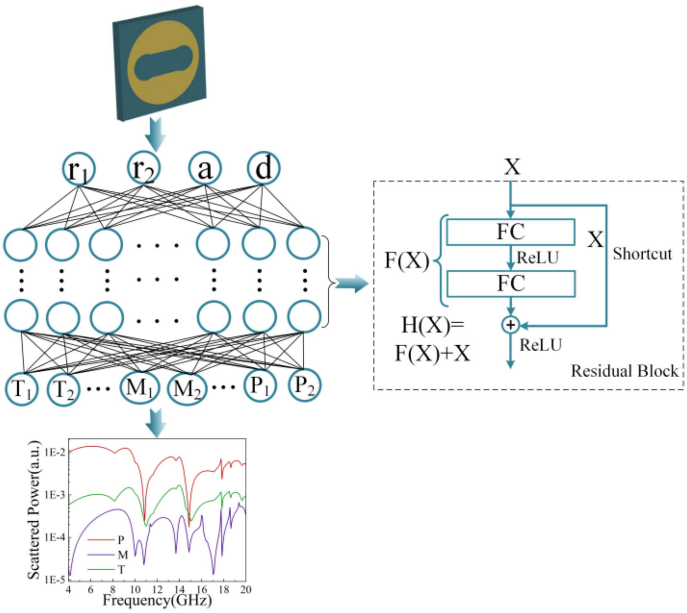

Fig. 2. The two network architectures of FNN which is consisted with the fully connected network (left) and residual blocks (right) respectively. We take the four special parameters of the metasurface as the input of deep learning. The deep learning network has six hidden layers, and each layer has a same of neurons.

the dimension and simplify the design process, only three main multipole scattering, ED, MD and TD, are considered in this study.

To save sampling time, the structural parameters are sampled at equal intervals using a joint simulation of CST and Python, and the scattered spectrum is discretized into 201 equally spaced points. In addition, the scattering spectra are processed with a logarithmic function in order to improve the predictive and inverse design capabilities of the network. Ultimately, a total of 2330 pairs of datasets are collected as the datasets for FNN and RNN, and each entry of the datasets constitutes four structural parameters and 201 spectral points of each of ED, MD and TD scattered spectra at a frequency range from 4 to 20 GHz. Furthermore, 80% of the total samples are randomly selected from the datasets as the training set, while the remaining 20% samples are divided into validating (10%), and test data sets (10%). The validation set is used to evaluate the network after each training epoch to avoid overfitting problems and determine the best iteration number. After the training with the training set, the network is checked by the test set. This analysis is done by comparing the loss maps between the true and predicted values.

III. Deep Learning Models

A. Forward Neural Network

To achieve the forward prediction of the metasurface, we have separately trained two network models with fully connected layers and residual blocks. The fully connected neural network structure is constructed as shown in the left of Fig. 2 and the other network has introduced with residual blocks as shown in the right of Fig. 2. Forward neural network (FNN) aims to learn mapping from structural parameters to scattering properties (EDs, MDs and TDs) by training with a small amount of data, so that the scattering energies can be accurately predicted from a given metasurface. Thus, the structural parameters are used as inputs to the FNN, while the three scattered powers of ED, MD and TD are output as results. The entire FNN consists of fully connected (FC) layers including an input layer, an output layer and six hidden layers.

TABLE II
The Results of Two Network Models

Models	Train Loss	Test loss	Time(min)
FC	0.026	0.034	25
Residual block	0.012	0.025	12

At the same time, residual blocks of deep residual learning framework are introduced as hidden layers to avoid the degradation problem that occurs with increasing network depth [31]. The number of neurons in each layer is set to the same 603 to ensure that the input X of the shortcut connections to match the dimension of F(X). Each weight layer, except the output layer, is nonlinearized with Rectified Linear Unit (ReLU). During training, the network model is evaluated with a loss function, which is usually expressed the difference between the predicted value and the true value. The smaller the difference, the better the fit of the network model. In the network, the loss function is defined with the mean square error (*MSE*) from the follow:

$$MSE = \frac{\sum_{i=1}^{n} (S_{pre} - S_{sim})^2}{n} \tag{5}$$

where n is the number of samples in the calculation process, S_{pre} is the scattered spectrum predicted by the neural network and S_{sim} is the true spectrum given during training.

Besides, the optimizer Adam [32] is used in the training to update the weights through the error back propagation process to minimize the *MSE*. The training set is used to train the FNN model, and after training, the test set consisted of samples that have never been used in previous training steps has been used to evaluate the model. Finally, we trained both the network models with the same dataset, the number of hidden layers and the same set of hyperparameters. And after 600 epochs, the results are shown in the Table II.

As can be seen from the Table II, the training loss of the network with the residual blocks is significantly lower than that of the fully connected network by more than half, and the error on the test set is 0.025 which is also much lower than 0.034 that of the fully connected network indicating that the network with residuals is able to predict the metasurface scattering spectrum better. At the same time, the training process of the residual network takes only 12 minutes, compared to 25 minutes for the fully connected network, which makes the residual network more efficient. Explicitly, the *MSE* of the training set can be minimized to 0.012 and the *MSE* of the test set reaches 0.025. The maximum *MSE* of the training set and test set are 0.087 and 0.156, respectively. Therefore, the residual network was chosen as the FNN in the manuscript for the prediction of the

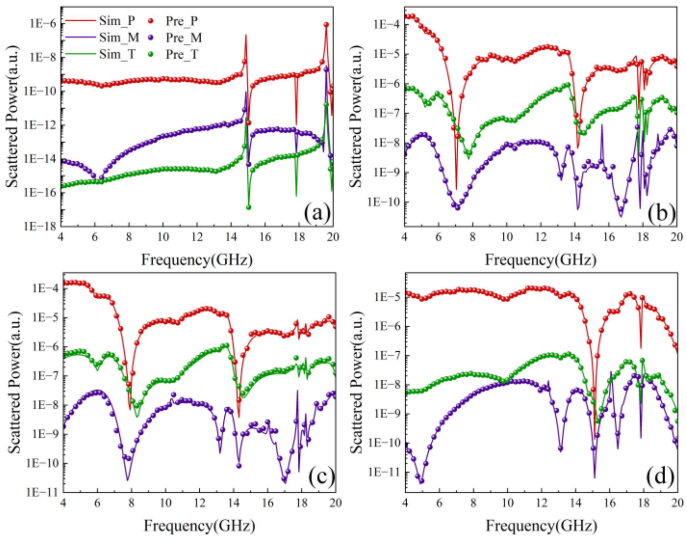

Fig. 3. Evaluation of the FNN model. The solid line represents the result obtained by CST simulation of the pre-selected structural parameters. The circles represent the result obtained by the structural parameters predicted by the FNN model; ED (red), MD (purple) and TD (green).

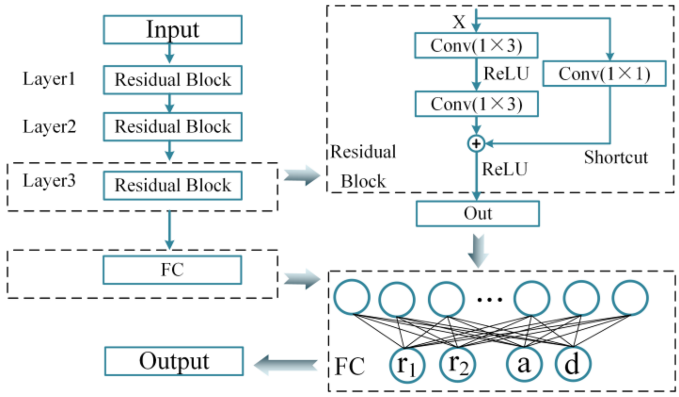

Fig. 4. Schematic diagram of RNN which is consisted with one-dimensional convolutional residual network and two fully connected layers are joined after the convolutional layer. The 201 spectral points of each ED, MD and TD scattered spectra have been taken as the input of RNN and the four geometrical parameters have been taken as outputs.

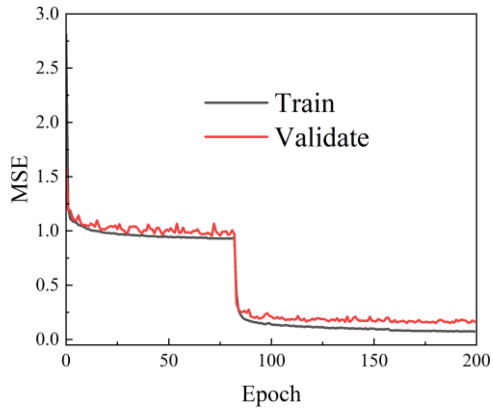

Fig. 5. The learning curve of the RNN.

metasurface scattered spectra. And from the statistics, it can claim that the proposed model FNN with the residual blocks can learn well from the datasets and predict the scattered powers of ED,MD and TD properly via the geometrical parameters.

For more intuitive illustration of the function, a set of the structural parameters of TD metasurface are freely chosen to obtain the corresponding scattering spectra through the prediction of FNN and the numerical calculation of CST respectively, and the results have been compared as shown in Fig. 3. The comparison of the results shows that the FNN is well trained to provide the scattering spectra of ED,MD and TD, which is very similar to the simulation results for the given input structural parameters. Compared with conventional methods for calculating electromagnetic multipole scattering, the proposed network structure, once trained, is able to quickly predict the scattering spectra of ED, MD and TD within a few seconds. Therefore, this method can replace the traditional electromagnetic simulation and scattered energy calculation and the designer can obtain the excitation patterns of an arbitrary TD metasurface in a short time.

B. Reverse Neural Network

In order to solve the inverse design problem of TD metasurfaces, a reverse neural network (RNN) is constructed for the fast design. As shown in the Fig. 4, the RNN consists of five layers of processing units and the main function is to automatically design TD metasurface with specific TD scattered power. The first three layers are composed of residual blocks which can be used for feature extraction of scattered powers of ED, MD and TD. The respective residual block contains three one-dimensional convolutional layers, and which one is a linear projection performed by the shortcut connection as shown in Fig. 4. The last two layers are all fully connected layers which are used to reduce the output dimension to generate the eventual output data. The kernel size is 1×3, except for the convolutional layer in shortcut connections, where the kernel size is 1×1. Similarly, each weight layer is nonlinearized with the ReLU activation function. And the output of the Layer3 is then flattened to be fed to the fully connected layers from 250 dimensions to 4 dimensions which generates the corresponding structural parameters of the TD metasurface. The activation function ReLU is also associated with the output layer to ensure the output is positive. The loss function is the MSE between the predicted structural parameters and the target structural parameters.

In order to improve the convergence rate, mini-batching is used to help the RNN model not be trapped in local minima [33]. The optimized hyperparameters used in RNN are the learning rate of 0.001 and a batch size of 20 respectively. Subsequently, the training of RNN is completed via the training set and the variation tendency of *MSE*s of the RNN during this training process has been shown in Fig. 5 and the *MSE* is the mean square error between the output values of structure parameters with the true. As can be seen from Fig. 5, the *MSE* on the training and validating sets gradually decreases as the number of the epoch increases and reaches the minimum values of 0.074 and 0.16 respectively at 200 epochs without overfitting problems.

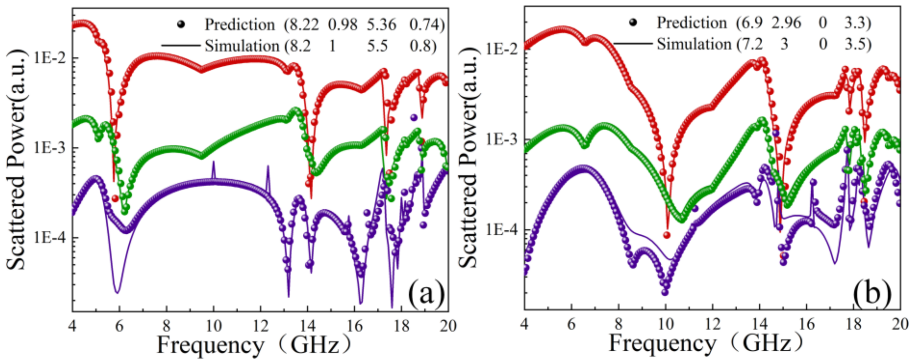

Fig. 6. Test examples of the RNN inverse design using the samples in test set. The target scattered spectra (solid lines) and the scattered responses (circles) obtained from the predicted design parameters; ED (red), MD (purple) and TD (green).

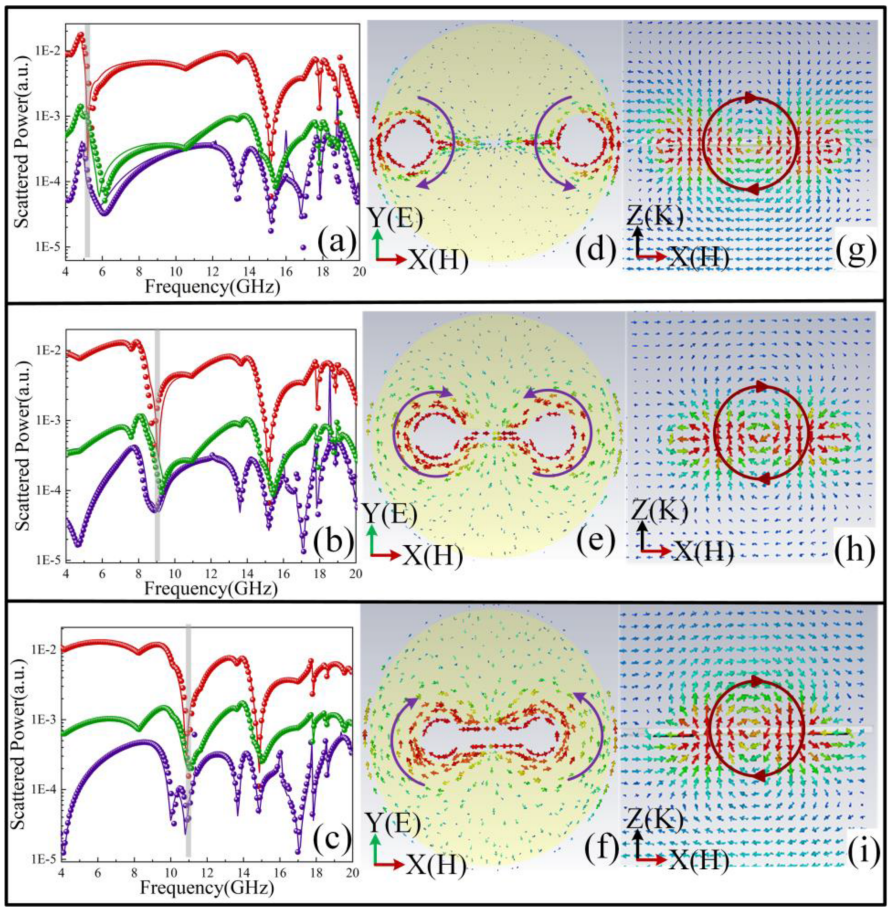

Fig. 7 (a)–(c) Spectra of random targets (solid lines) and the responses of the predicted TD metasurfaces (circles); ED (red), MD (purple) and TD (green). (d)–(i) the surface current and magnetic field distributions of the predicational toroidal metamaterial.

In addition, the average *MSE* between predicted and target responses of 233 test data sets is 0.18 quantitatively showing that RNN indeed provide appropriate designs that have desired optical properties.

As shown in Fig. 6, two examples of test results show that the predicted parameters (8.2, 1, 5.5, 0.8 and 7.2, 3, 03.5) are very close to the target metasurface (8.22, 0.98, 5.36, 0.74 and 6.9, 2.96, 0, 3.13). And the ED, MD and TD scattered powers obtained from predicted designs (circles) show good agreement with desired spectra (solid lines), especially for the TD and MD responses. Therefore, it can be considered that the proposed RNN is well trained to inversely design the parameters of TD metasurface properly according to the target ED, MD and TD responses.

Deep-learning-based inverse design is practically utilized to find a structure, which reconstructs an input spectrum with

specific purposes. To demonstrate the ability of the proposed network to inversely design TD metasurfaces using user- required spectra, metasurfaces with arbitrary TD resonances are engineered. As shown in the gray band in the solid line of Fig. 7, the scattered spectrums with arbitrary TD resonances are used as input of the method to automatically design the metasurfaces. It takes only 2 seconds to batch design three user-required metasurfaces, which is much faster than the parameter optimization process of previous work [34]. The parameters of the designed metasurfaces are (5.9, 1.37, 2.9, 0.3), (6.29, 1.35, 1.63, 0.69) and (7.15, 1.28, 1.63, 1.48) and the scattered spectra of ED, MD and TD obtained from the predicted designs after numerical calculations are shown as circles in Fig. 7. In addition, the *MSEs* between the required spectra with the calculated are 0.023, 0.016 and 0.012 respectively.

As can be seen from the Fig. 7, the results of RNN prediction are highly overlapping with the target scattering, and especially the trends of EDs and TDs scattering are well fitted with the given scattered spectra. Although there is a slight frequency shift at the intersection of ED and TD scattering, the TD scattering still remains dominant near the gray band. The accurate prediction at different resonant frequencies indicates that the method can achieve arbitrary TD resonance prediction at different target frequencies. In addition, the TD mode is further demonstrated by calculating the surface current and cross-sectional magnetic field distribution at the resonance. According to the Fig. 7(d)–(f), a pair of reverse flowing currents can be clearly observed independently which can form a head-to-tail magnetic field, that is the TD in the y-direction, as shown in Fig. 7(g)–(i).

To sum up, our networks model can make good predictions of TD metasurfaces and further decrease the time-consuming numerical simulations to calculate the scattered spectrums. Our proposed model cannot obtain the S parameters at the same time as the scattered spectrum is calculated. However, if a large relevant dataset of metamaterials with S parameters is available, the model will be able to get the connection between the scattered spectra and S parameters, and successfully predict accurate TD results.

IV. Conclusion

In conclusion, a method had been provided to inverse design the structural parameters of TD metasurfaces based on independently given ED, MD and TD spectra. Firstly, a forward prediction network is designed with a fully connected network based on residuals. After training, the scattered power can be predicted according to the structural parameters provided by the user quickly and approximates the numerical calculation results with high accuracy. In addition, a convolutional residual network is proposed for the inverse design of TD metasurfaces. To show the capability of the RNN, a deep-learning-assisted inverse design for TD resonance are specifically demonstrated.

Using this model to reversely design the TD metasurface avoids the highly non-linear problem of solving the Maxwell equation and the large amount of time wasted in traditional numerical calculation methods which can predict the appropriate structural parameters to meet user requirements based on an arbitrary scattered power spectrum. We believe that the proposed efficient inverse design method will provide new ideas for the design and development of TD metasurfaces in the future.

References

[1] I. Zel'Dovich, "Electromagnetic interaction with parity violation," *Sov. J. Exp. Theor. Phys.*, vol. 6, pp. 1184–1186, 1958.

[2] T. Chen, T. Xiang, J. Wang, T. Lei, and F. Lu, "Double E-shaped toroidal metasurface with high Q-factor Fano resonance and electromagnetically induced transparency," *AIP Adv.*, vol. 11, no. 9, Sep. 2021, Art. no. 095011.

[3] T. A. Raybould et al., "Toroidal circular dichroism," *Phys. Rev. B*, vol. 94, no. 3, pp. 2–6, 2016.

[4] X. Luo, X. Li, T. Lang, X. Jing, and Z. Hong, "Excitation of high Q toroidal dipole resonance in an all-dielectric metasurface," *Opt. Mater. Exp.*, vol. 10, no. 2, pp. 358–368, 2020.

[5] T. Lei, T. Xiang, J. Wang, R. Zhou, and X. Zhu, "Dual-toroidal analog EIT with metamaterial," *Appl. Phys. Exp.*, vol. 14, no. 6, Jun. 2021, Art. no. 067001.

[6] S. Wang, S. Wang, X. Zhao, J. Zhu, Q. Li, and T. Chen, "Excitation of electromagnetically induced transparency effect in asymmetrical planar terahertz toroidal dipole metasurfaces," *J. Infrared, Millimeter, Terahertz Waves*, vol. 42, no. 1, pp. 40–49, 2021.

[7] T. Kaelberer, V. A. Fedotov, N. Papasimakis, D. P. Tsai, and N. I. Zheludev, "Toroidal dipolar response in a metamaterial," *Science*, vol. 330, no. 6010, pp. 1510–1512, Dec. 2010.

[8] Z. Shen et al., "Electromagnetically induced transparency metamaterial with strong toroidal dipole response," *Mater. Res. Exp.*, vol. 7, no. 3, Mar. 2020, Art. no. 035802.

[9] D. Yan, M. Meng, J. Li, and X. Li, "Graphene-assisted narrow bandwidth dual-band tunable terahertz metamaterial absorber," *Front. Phys.*, vol. 8, Aug. 2020. Art. no. 306.

[10] A. Bhattacharya, K. M. Devi, T. Nguyen, and G. Kumar, "Actively tunable toroidal excitations in graphene based terahertz metamaterials," *Opt. Commun.*, vol. 459, Nov. 2019, Art. no. 124919.

[11] Y. Chen and Y. Wang, "Electrically tunable toroidal Fano resonances of symmetry-breaking dielectric metasurfaces using graphene in the infrared region," *J. Opt.*, vol. 24, no. 4, Apr. 2022, Art. no. 044012.

[12] A. Ahmadivand et al., "Rapid detection of infectious envelope proteins by magnetoplasmonic toroidal metasensors," *ACS Sensors*, vol. 2, no. 9, pp. 1359–1368, 2017.

[13] Y. Sun et al., "Toroidal dipole and magnetic multipole excitations from the same nanostructure with different direction of electric dipole emitters," *Appl. Phys. A Mater. Sci. Process.*, vol. 126, no. 3, pp. 1–7, 2020.

[14] Q. Wu et al., "Comparison of different neural network architectures for plasmonic inverse design," *ACS Omega*, vol. 6, no. 36, pp. 23076–23082, Aug. 2021.

[15] I. Malkiel, M. Mrejen, A. Nagler, U. Arieli, L. Wolf, and H. Suchowski, "Plasmonic nanostructure design and characterization via deep learning," *Light Sci. Appl.*, vol. 7, no. 1, Sep. 2018. Art. no. 60 .

[16] X. Xu, C. Sun, Y. Li, J. Zhao, J. Han, and W. Huang, "An improved tandem neural network for the inverse design of nanophotonics devices," *Opt. Commun.*, vol. 481, Feb. 2021, Art. no. 126513.

[17] Q. Zhang et al., "Machine-learning designs of anisotropic digital coding metasurfaces," *Adv. Theory Simul.*, vol. 2, no. 2, pp. 1–13, 2019.

[18] H. Lin et al., "Machine-learning-assisted inverse design of scattering enhanced metasurface," *Opt. Exp.*, vol. 30, no. 2, 2022, Art. no. 3076.

[19] L. Li, H. Zhao, C. Liu, L. Li, and T. J. Cui, "Intelligent metasurfaces : Control, communication and computing," *eLight*, vol. 2, no. 1, May 2022. Art. no. 7.

[20] Y. Deng, S. Ren, K. Fan, J. M. Malof, and W. J. Padilla, "Neural-adjoint method for the inverse design of all-dielectric metasurfaces," *Opt. Exp.*, vol. 29, no. 5, 2021, Art. no. 7526.

[21] J. Ma et al., "Inverse design of broadband metasurface absorber based on convolutional autoencoder network and inverse design network," *J. Phys. D. Appl. Phys.*, vol. 53, no. 46, Nov. 2020, Art. no. 464002.

[22] J. Noh et al., "Design of a transmissive metasurface antenna using deep neural networks," *Opt. Mater. Exp.*, vol. 11, no. 7, Jul. 2021, Art. no. 2310.

[23] J. Ines, N. Ammar, T. Aguili, and H. Baudrand, "An efficient algorithm for electromagnetic scattering by a set of perfect conducting cylindrical objects using the artificial neural network," *Int. J. RF Microw. Comput. Eng.*, vol. 29, no. 4, pp. 1–12, 2019.

[24] S. So, Y. Yang, T. Lee, and J. Rho, "On-demand design of spectrally sensitive multiband absorbers using an artificial neural network," *Photon. Res.*, vol. 9, no. 4, pp. B153–B158, Apr. 2021.

[25] F. Ghorbani, J. Shabanpour, S. Beyraghi, H. Soleimani, H. Oraizi, and M. Soleimani, "A deep learning approach for inverse design of the metasurface for dual-polarized waves," *Appl. Phys. A Mater. Sci. Process.*, vol. 127, no. 11, pp. 1–7, 2021.

[26] W. Huang, Z. Wei, B. Tan, S. Yin, and W. Zhang, "Inverse engineering of electromagnetically induced transparency in terahertz metamaterial via deep learning," *J. Phys. D Appl. Phys.*, vol. 54, no. 13, Apr. 2021, Art. no. 135102.

[27] B. G. DeLacy, J. D. Joannopoulos, M. Tegmark, and M. Soljačić, "Nanophotonic particle simulation and inverse design using artificial neural networks," *Sci. Adv.*, vol. 4, no. 6, pp. 1–8, Jun. 2018.

[28] S. So, J. Mun, and J. Rho, "Simultaneous inverse design of materials and structures via deep learning: Demonstration of dipole resonance engineering using core–shell nanoparticles," *ACS Appl. Mater. Interfaces*, vol. 11, no. 27, pp. 24264–24268, 2019.

[29] D. A. Smirnova et al., "Enhanced light-matter interactions in dielectric nanostructures via machine-learning approach," *Adv. Photon.*, vol. 2, no. 2, pp. 1–11, 2020.

[30] V. A. Fedotov, A. V. Rogacheva, V. Savinov, D. P. Tsai, and N. I. Zheludev, "Resonant transparency and non-trivial non-radiating excitations in toroidal metamaterials," *Sci. Rep.*, vol. 3, pp. 1–5, 2013.

[31] K. He, X. Zhang, S. Ren, and J. Sun, "Deep residual learning for image recognition," in *Proc. IEEE Comput. Soc. Conf. Comput. Vis. Pattern Recognit.*, 2016, pp. 770–778.

[32] D. P. Kingma and J. L. Ba, "Adam: A method for stochastic optimization," in *Proc. 3rd Int. Conf. Learn. Represented Track*, 2015, pp. 1–15.

[33] H. T. Kollmann, D. W. Abueidda, S. Koric, E. Guleryuz, and N. A. Sobh, "Deep learning for topology optimization of 2D metamaterials," *Mater. Des.*, vol. 196, 2020, Art. no. 109098.

[34] T. Xiang, T. Lei, T. Chen, Z. Shen, and J. Zhang, "Low-loss dual-band transparency metamaterial with toroidal dipole," *Mater. (Basel)*, vol. 15, no. 14, Jul. 2022, Art. no. 5013.